Bulletin of Electrical Engineering and Informatics
Vol. x, No. x, December 202x, pp. xx∼xx
ISSN: 2302-9285, DOI: 10.11591/eei.vxix.yyyy

Outage Performance Analysis of NOMA over Log-Normal Fading distribution in presence of CSI and SIC imperfections

Chi-Bao Le[1], Cuu-Ho Van[2], Hong-Nhu Nguyen[2], Nguyen Thi Hau[2], Nhan Duc Nguyen[3]
[1]Faculty of Electronics Technology, Industrial University of Ho Chi Minh City (IUH), Ho Chi Minh City, Vietnam
[2]Faculty of Electronics and Telecommunications, Saigon University (SGU), Ho Chi Minh City, Vietnam
[3]Innovation Center, Van Lang University, Ho Chi Minh City, Vietnam

Article Info

Article history:

Received Jun 9, 2018
Revised Nov 20, 2018
Accepted Dec 11, 2018

Keywords:

NOMA
log-normal fading
outage probability
imperfect CSI
imperfect SIC

ABSTRACT

The evolution of wireless communication networks has introduced various applications that requires massive device connectivity and high spectral efficiency. Non-orthogonal multiple access (NOMA) technique has proved to be highly efficient and one of the most promising technology to perform efficient data transmission through the network. The NOMA technique has the ability to allocate same resource block for two users by superimposing their data signals. At the receiver, the signals are separated by performing successive interference cancellation (SIC) technique. For efficient data transmission, the fading and shadowing effects of channels also play a pivotal role. Many researches have considered Rayleigh, Rician, Nakagami-m and other fading channels in various perspectives. In our paper, we propose a system model based on NOMA network with two users over log-normal fading distribution in presence of channel estimation errors and SIC imperfections. The performance was anlaysed in terms of outage probability and simulations were performed in assistance with Monte-Carlo simulations. The obtained results are shown to be effective in comparison to traditionally used fading distributions. The same analysis is also performed in various scenarios of power allocation level, target rates and imperfections. Finally, it is understood that transmit SNR and power allocation of the users are important for efficient communication in any fading distribution as shown in this paper.

Corresponding Author:

Nhan Duc Nguyen
Innovation Center, Van Lang University, Ho Chi Minh City, Vietnam
Email: nhan.nd@vlu.edu.vn.

1. INTRODUCTION

The introduction of non-orthogonal multiple access (NOMA) technique have paved way for massive device connectivity among the network. NOMA has become the most viable option to be implemented in 4th generation (4G) networks and beyond [1]. NOMA has the ability to serve multiple users in the same cluster using the same resources. It transmits the signal by superimposing the users signals, which also leads to improved spectral efficiency. At the receiver, the superimposed signals are separated by performing successive interference cancellation. During the signal transmission, the channel state information (CSI) of the users might be known or unknown. The implementation and integration of NOMA with various emerging and trending technologies and techniques has become mandatory to achieve efficient results in various system models. One of most important parameters to be considered for a quality signal transmission is its fading channel distribution. There are various number of fading channels such as Rayleigh, Rice, Rician, Nakagami-m, etc., which are proved to be efficient in the radio environment when optimized.

1.1. Related work

In [2], the authors have considered downlink cooperative NOMA (C-NOMA) network under Nakagami-m fading channels to investigate the outage performance and sum-rate of the system. Similar system was considered in [3] in presence of Rician fading channel and the performance was evaluated in terms of achievable rate. In [4], the authors have proposed a downlink and uplink NOMA network over Rayleigh fading channel in presence of SIC errors. The performance of the system was evaluated in terms of bit error rate (BER). In [5], the authors have investigated the performance of NOMA2000 and power domain NOMA (P-NOMA) and the compared results shows that P-NOMA has yielded better results than NOMA2000. Different from the remaining articles, the authors in [6] have considered generalized fading channels $(\eta - \mu)$ and $(\kappa - \mu)$ in a downlink NOMA network. The performance was investigated in terms of outage probability by keeping the fixed target rate. When the results are compared with OMA, NOMA, shows the better performance rate. Also it is noticed that the performance keeps getting better with the increase in signal-to-noise ratio (SNR). Similar with [2], the outage performance of C-NOMA was investigated over log-normal fading distribution in [7]. Secrecy performance was investigated on similar model in [8]. NOMA has also been integrated with various technologies which has improved its operational efficiency. In [9], the authors have proposed reconfigurable intelligent surfaces (RIS)-assisted C-NOMA in both half duplex and full duplex modes. The authors have proposed an efficient algorithm to minimize the power consumption at both base station and the receiver. Visible light communication (VLC) is also another emerging technology which has immense capacity to perform quality signal transmission underwater. In [10], the authors have employed VLC-based wireless sensor network using NOMA technique to perform system capacity analysis over log-normal distribution. Meanwhile in [11], the authors integrated millimetre Wave (mmWave) with NOMA to achieve massive device connectivity and improved data transmission secrecy. The authors have proposed two schemes based on joint user grouping and power optimization which are shown to be efficient in enhancing the system performance. The presence of single and multiple eavesdropper scenario was considered in [12] to analyse the performance of NOMA network in ground-to-air communications. The performance was investigated in terms of secrecy outage probability (SOP).

In [13], the authors have proposed integration of RIS with NOMA technique, aiming to minimize the transmit power by optimizing the order of users, beamforming vectors and phase shift matrix. The authors have proposed a difference-of-convex algorithm to solve non-convex problems and an efficient user-ordering scheme to enhance the target data rates. Similar system design was proposed in [14] to optimize the rate performance and user fairness in the network. Efficient algorithms were proposed to deal with the non-convex algorithms and obtained results are comparatively efficient than traditional system models. Whereas in [15], multiple RIS-assisted NOMA network in presence of discrete phase shifts are investigated to enhance the signal quality of each user present in the network. Direct link and no direct link with each user scenarios were considered and the performance was analysed in terms of outage probability. In [16], NOMA-assisted vehicle-to-everything (V2X) communications was proposed in presence of back-scattering to enhance the achievable rates through cooperation between the devices. Optimal power allocation schemes were introduced in the network to enhance the communication between the base station and road side units that acts as a bridge for vehicles to communicate. In scenario of industrial IoT, NOMA technique is proposed to enhance the connectivity of number of ultra reliable low latency (URLLC) devices in [17]. The proposed model allows multiple URLLCs to keep connected and transmit data simultaneously across the multiple frequency channels. The performance of each user pair or cluster is analysed in terms of achievable sum rates. The studies provides important inputs to the research as the each paper provides detailed performances of the system in various scenarios. In the perspective of real-world implementations, most of the research works considered only ideal cases such as perfections in all parameters. Therefore, this research has different perspective and our considered model will be approximate to the real-world implementation.

1.2. Motivation and Organization

As mentioned, most of the research works are based on the ideal case situations which are meant to be changed when implemented in the real-world. Therefore, we are motivated to analyse the performance of below proposed model while it is facing few imperfections during the transmission process. It is important to understand and investigate the performance of various models. As of the above studies, NOMA has been studied in various fading environments such as Rayleigh, Rician, log-normal, etc. But, particularly in log-normal, there is no dedicated study to analyse its performance in presence of channel estimation errors and

imperfect SIC. Therefore, in this paper, we propose a model based on NOMA network over log-normal fading distribution in presence of both perfect and imperfect SIC. The performance of the system was studied in term of outage probability and in-depth discussions are provided in the following sections. The major contributions of this paper is as follows:

- Deriving closed-form outage probability expressions for the proposed model in presence of channel estimation errors and imperfect SIC.
- Computing the throughput expression basing on the outage probability expressions derived.
- Simulating the expression in MATLAB in assistance with Monte-Carlo simulation verifying the authenticity of obtained expressions.
- Analysing the effects of channel estimation errors and imperfect SIC in NOMA network over log-normal fading effect.

The remaining of the paper is as follows: Section 2 introduces and describes the system model and its characteristics. Section 3 provides the computations based on outage probability and section 4 provides the computations for throughput of the system. Section 5 provides the numerical analysis with simulations and indepth discussions on it. Finally, section 6 concludes the paper.

2. SYSTEM MODEL AND CHANNEL CHARACTERISTICS

2.1. System Model

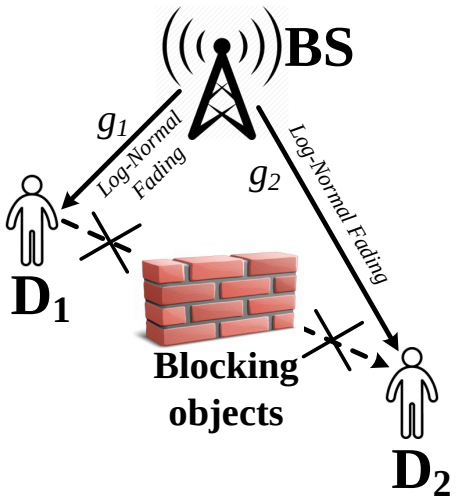

Figure 1. System model of downlink two users NOMA

As shown in Figure 1, we consider a NOMA network in presence of a base station (BS) communicating with two users D_1 and D_2, with single antennas at both users, which does not any direct link between the two users. The considered links, from BS to users, are estimated to be following log-normal fading with channel coefficients g_1 and g_2 at respective users. Due to imperfect CSI, the estimated channel gains of the relay-user links are given as [18]

$$\hat{h}_j = h_j + e_j \quad , j \in \{1, 2\} \tag{1}$$

where $e_j \sim \mathcal{CN}(0, \Omega_e)$ is the channel estimation error and h_j is the estimated channel coefficients [19].

The received signal at the two NOMA users, D_1 and D_2 are given by [20]

$$y_1 = \hat{h}_1\sqrt{P_S}\left(\sum_{j=1}^{2}\sqrt{\nu_j}x_j\right) + \omega_1 = (h_1 + e_1)\sqrt{P_S}\left(\sum_{j=1}^{2}\sqrt{\nu_j}x_j\right) + \omega_1 \quad , \tag{2a}$$

$$y_2 = \hat{h}_2\sqrt{P_S}\left(\sum_{j=1}^{2}\sqrt{\nu_j}x_j\right) + \omega_2 = (h_2 + e_2)\sqrt{P_S}\left(\sum_{j=1}^{2}\sqrt{\nu_j}x_j\right) + \omega_2 \quad , \tag{2b}$$

where P_S denotes the normalized transmission power at the base station (BS), ω_1 and ω_2 denotes the additive white Gaussian noise (AWGN) at the node D_1 and D_2, respectively, and x_j is assumed to be normalised the unity power signal for the j-th user, i.e., $\mathbb{E}\left\{x_j^2\right\} = 1$ in which $\mathbb{E}$ is the Expectation operator. The j-th user's power allocation factor ν_j satisfies the relationship $\nu_2 > \nu_1$ with $\sum_{j=1}^{2}\sqrt{\nu_j} = 1$, which is for the sake of user fairness. Meanwhile, the noise terms are additive white Gaussian noise (AWGN) with zero mean and variance of N_0

In the first phase, the signal to interference-plus-noise ratio (SINR) after treating x_1 as interference is given by

$$\Gamma_{D_1,x_2} = \frac{\nu_2\rho_S|h_1|^2}{1 + \rho_S\Omega_e + \nu_1\rho_S|h_1|^2} = \frac{\nu_2\rho_S\gamma_1}{1 + \rho_S\Omega_e + \nu_1\rho_S\gamma_1}, \tag{3}$$

where $\gamma_i \triangleq |h_i|^2, i \in \{1, 2\}$ and the transmit signal to noise ratio (SNR) computed at the BS as $\rho_S = P_S/N_0$. Note that γ_1 and γ_2 are independent RVs

It is worth noting that imperfect SIC (ipSIC) occurs, the SINR of detect x_2 is given as [21]

$$\Gamma_{D_1,x_1}^{ipSIC} = \frac{\nu_1\rho_S\gamma_1}{1 + \rho_S\Omega_e + \rho_S|h_I|^2}, \tag{4}$$

where $|h_I|^2 \sim \mathcal{CN}(0, \lambda_I)$ in [22], with $\lambda_I\,(0 \le \lambda_I < 1)$ denotes as the level of residual interference caused by imperfect SIC and $\mathcal{CN} \sim (a, b)$ complex normal distribution with average a and variance b.

Similarly, the instantaneous SINR at D_2 to detect x_2 is given as

$$\Gamma_{D_2,x_2} = \frac{\nu_1\rho_S\gamma_2}{1 + \rho_S\Omega_e + \nu_2\rho_S\gamma_2}. \tag{5}$$

2.2. Channel Characteristics

Let $\sigma_{h,\mathrm{dB}}^2 = \sigma_{h_1,\mathrm{dB}}^2 = \sigma_{h_2,\mathrm{dB}}^2$ and $\mu_{h,\mathrm{dB}} = \mu_{h_1,\mathrm{dB}} = \mu_{h_2,\mathrm{dB}}$ are the mean and variances of $10\log h_i$, $i \in \{1, 2\}$, respectively. Now $\gamma = \gamma_1 = \gamma_2$ has log-normal fading probability density function (PDF), which is given by [23, Eq. (1)]

$$f_\gamma(x) = \frac{\xi}{x\sqrt{2\pi\sigma_{z_{h,\mathrm{dB}}}^2}} e^{-\frac{\left(\xi\ln x - \mu_{z_{h,\mathrm{dB}}}\right)^2}{2\sigma_{z_{h,\mathrm{dB}}}^2}}, \tag{6}$$

where $\xi = \frac{10}{\ln 10}$, $\ln x$ denote the natural logarithms, $\sigma_{z_{h,\mathrm{dB}}}^2 = \mathrm{var}\left(z_{h,\mathrm{dB}}\right) = 4\sigma_{h,\mathrm{dB}}^2$ and $\mu_{z_{h,\mathrm{dB}}} = E\left(z_{h,\mathrm{dB}}\right) = 2\mu_{h,\mathrm{dB}}$, $\mathrm{var}\,(x)$ and $E\,(x)$ denote the variance and the expectation, respectively.

The cumulative distribution functions (CDF) of γ can be obtained as

$$F_\gamma(x) = \int_0^x f_\gamma(y)\,dy = \frac{\xi}{\sqrt{2\pi\sigma_{z_{h,\mathrm{dB}}}^2}} \int_0^x \frac{1}{y} e^{-\frac{\left(\xi\ln y - \mu_{z_{h,\mathrm{dB}}}\right)^2}{2\sigma_{z_{h,\mathrm{dB}}}^2}} dy, \tag{7}$$

By the change of variable $t = \ln(y) \rightarrow dt = dy/y$ in (7), the CDF moments can be rewritten as

$$F_\gamma(x) = \frac{\xi}{\sqrt{2\pi\sigma_{z_{h,\mathrm{dB}}}^2}} \int_{-\infty}^{\ln x} e^{-\frac{\left(\xi t - \mu_{z_{h,\mathrm{dB}}}\right)^2}{2\sigma_{z_{h,\mathrm{dB}}}^2}} dt. \tag{8}$$

After some manipulations, the last integral can be rewritten as follows:

$$F_{\gamma}\left(x\right)=\frac{\xi}{2}\left[\mathrm{erf}\left(\frac{\xi\ln\mathrm{x}-\mu_{\mathrm{z_{h,dB}}}}{\sigma_{\mathrm{z_{h,dB}}}\sqrt{2}}\right)+1\right]=\frac{\xi}{2}\mathrm{erfc}\left(-\frac{\xi\ln\mathrm{x}-\mu_{\mathrm{z_{h,dB}}}}{\sigma_{\mathrm{z_{h,dB}}}\sqrt{2}}\right), \tag{9}$$

where $\mathrm{erfc}\left(x\right)=1-\mathrm{erf}\left(x\right)=\frac{2}{\sqrt{\pi}}\int_{x}^{+\infty}e^{-y^{2}}dy$ is the complementary error function in [24, Eq. (8.250.1)].

Following that, we have $\left|h_I\right|^2$'s PDF and CDF in [25]:

$$f_{\left|h_I\right|^2}\left(x\right)=\frac{1}{\lambda_I}e^{-\frac{x}{\lambda_I}}, \tag{10}$$

and

$$F_{\left|h_I\right|^2}\left(x\right)=1-e^{-\frac{x}{\lambda_I}}. \tag{11}$$

3. ANALYSIS OF OUTAGE PROBABILITY

First, the outage probability with imperfect SIC (ipSIC) of D_1 is calculated as

$$P_{D_1}^{ipSIC}=1-\Pr\left(\Gamma_{D_1,x_2}>\varepsilon_2,\Gamma_{D_1,x_1}^{ipSIC}>\varepsilon_1\right)=1-\Pr\left(\gamma_1>\delta_2,\gamma_1>\delta_1\left(\rho_S\left|h_I\right|^2+\ell_e\right)\right), \tag{12}$$

where $\varepsilon_i=2^{2R_i}-1$, for $i=1,2$ is called as target rate at D_i, $\ell_e=\left(\rho_S\Omega_e+1\right)$, $\delta_2=\frac{\varepsilon_2\ell_e}{\rho_S\left(\nu_2-\nu_1\varepsilon_2\right)}$ and $\delta_1=\frac{\varepsilon_1}{\nu_1\rho_S}$. Assuming $\delta_1\left(\rho_S\left|h_I\right|^2+\ell_e\right)\gg\delta_2$, OP_1 can be calculated by

$$\begin{aligned}P_{D_1}^{ipSIC}=&1-\Pr\left(\gamma_1>\delta_1\left(\rho_S\left|h_I\right|^2+\ell_e\right)\right)\\=&1-\int_0^{\infty}f_{\left|h_I\right|^2}\left(x\right)\left[1-F_{\gamma_1}\left(\delta_1\left(\rho_S x+\ell_e\right)\right)\right]dx.\end{aligned} \tag{13}$$

We using PDF of (10) and CDF of (9), (13) is given as

$$\begin{aligned}P_{D_1}^{ipSIC}=&1-\int_0^{\infty}f_{\left|h_I\right|^2}\left(x\right)\left[1-F_{\gamma_1}\left(\delta_1\left(\rho_S x+\ell_e\right)\right)\right]dx\\=&1-\frac{1}{\lambda_I}\int_0^{\infty}e^{-\frac{x}{\lambda_I}}\left[1-\frac{\xi}{2}\mathrm{erfc}\left(-\frac{\xi\ln\left(\delta_1\left(\rho_S\mathrm{x}+\ell_e\right)\right)-\mu_{\mathrm{z_{h,dB}}}}{\sigma_{\mathrm{z_{h,dB}}}\sqrt{2}}\right)\right]dx\\=&\frac{\xi}{2\lambda_I}\int_0^{\infty}e^{-\frac{x}{\lambda_I}}\mathrm{erfc}\left(-\frac{\xi\ln\left(\delta_1\left(\rho_S\mathrm{x}+\ell_e\right)\right)-\mu_{\mathrm{z_{h,dB}}}}{\sigma_{\mathrm{z_{h,dB}}}\sqrt{2}}\right)dx.\end{aligned} \tag{14}$$

Let $r=\frac{4}{\pi}\arctan\left(x\right)-1\Rightarrow\tan\left(\frac{\pi(r+1)}{4}\right)=x\Rightarrow\frac{\pi}{4}\sec^2\left(\frac{\pi}{4}\left(r+1\right)\right)dr=dx$ in which $\sec^2\left(x\right)=\frac{1}{\cos^2(x)}$, $P_{D_1}^{ipSIC}$ is given as

$$\begin{aligned}P_{D_1}^{ipSIC}=&\frac{\xi}{2\lambda_I}\int_0^{\infty}e^{-\frac{x}{\lambda_I}}\mathrm{erfc}\left(-\frac{\xi\ln\left(\delta_1\left(\rho_S\mathrm{x}+\ell_e\right)\right)-\mu_{\mathrm{z_{h,dB}}}}{\sigma_{\mathrm{z_{h,dB}}}\sqrt{2}}\right)dx\\\overset{a}{=}&\frac{\pi\xi}{8\lambda_I}\int_{-1}^{1}\sec^2\left(\frac{\pi}{4}\left(r+1\right)\right)e^{-\frac{1}{\lambda_I}\tan\left(\frac{\pi(r+1)}{4}\right)}\mathrm{erfc}\left(-\frac{\xi\ln\left(\rho_S\delta_1\tan\left(\frac{\pi(\mathrm{r}+1)}{4}\right)+\ell_e\delta_1\right)-\mu_{\mathrm{z_{h,dB}}}}{\sigma_{\mathrm{z_{h,dB}}}\sqrt{2}}\right)dr.\end{aligned} \tag{15}$$

Though it is difficult to derive a closed-form expression for (15), we can obtain an accurate approximation for it. In step (a) is achieved by applying the Gaussian-Chebyshev quadrature [26, Eq. (25.4.38)]. Now

we have $P_{D_1}^{ipSIC}$ is given by

$$\begin{aligned} P_{D_1}^{ipSIC} \approx & \frac{\pi^2 \xi}{8K\lambda_I} \sum_{k=1}^{K} \sqrt{1-\xi_k^2} \sec^2\left(\pi 4^{-1}\left(\xi_k+1\right)\right) e^{-\frac{\tan\left(\pi 4^{-1}\left(\xi_k+1\right)\right)}{\lambda_I}} \\ & \times \operatorname{erfc}\left(-\frac{\xi \ln\left(\rho_S \delta_1 \tan\left(\pi 4^{-1}\left(\xi_k+1\right)\right)+\ell_e \delta_1\right)-\mu_{z_{h,\mathrm{dB}}}}{\sigma_{z_{h,\mathrm{dB}}}\sqrt{2}}\right), \end{aligned} \tag{16}$$

where $\xi_k = \cos\left(\frac{2k-1}{K}\pi\right)$.

Specifically, assume $\lambda_I \to 0$ then $|h_I|^2 \approx 0$, we have the outage probability with pefect SIC (pSIC) $P_{D_1}^{pSIC}$ is calculated as

$$\begin{aligned} P_{D_1}^{pSIC} =& 1-\Pr\left(\frac{\nu_2 \rho_S \gamma_1}{1+\ell_e+\nu_1 \rho_S \gamma_1} > \varepsilon_2, \nu_1 \rho_S \gamma_1 > \ell_e \varepsilon_1\right) \\ =& 1-\Pr\left(\gamma_1 > \delta_2, \gamma_1 > \ell_e \delta_1\right) \\ =& 1-\Pr\left(\gamma_1 > \delta_{\max}\right), \end{aligned} \tag{17}$$

where $\delta_{\max} = \max(\delta_2, \ell_e \delta_1)$. With the help of (9), $P_{D_1}^{pSIC}$ is given as

$$\begin{aligned} P_{D_1}^{pSIC} =& 1-\Pr\left(\gamma_1 > \delta_{\max}\right) \\ =& F_{\gamma_1}\left(\delta_{\max}\right) \\ =& \frac{\xi}{2} \operatorname{erfc}\left(-\frac{\xi \ln \delta_{\max}-\mu_{\mathrm{z_{h,dB}}}}{\sigma_{\mathrm{z_{h,dB}}}\sqrt{2}}\right) \end{aligned} \tag{18}$$

Finally, similar to P_{D_1} the outage probability of D_2 is calculated as

$$\begin{aligned} P_{D_2} =& 1-\Pr\left(\Gamma_{D_2,x_2} > \varepsilon_2\right) \\ =& 1-\Pr\left(\frac{\nu_1 \rho_S \gamma_2}{1+\ell_e+\nu_2 \rho_S \gamma_2} > \varepsilon_2\right) \\ =& 1-\Pr\left(\gamma_2 > \delta_2\right) \\ =& F_{\gamma_2}\left(\delta_2\right) \\ =& \frac{\xi}{2} \operatorname{erfc}\left(-\frac{\xi \ln \delta_2-\mu_{z_{h,\mathrm{dB}}}}{\sigma_{z_{h,\mathrm{dB}}}\sqrt{2}}\right). \end{aligned} \tag{19}$$

4. SYSTEM THROUGHPUT ANALYSIS

$$\tau_{sys}^{ipSIC} = \left(1-P_{D_1}^{ipSIC}\right) R_1 + \left(1-P_{D_2}\right) R_2, \tag{20a}$$

$$\tau_{sys}^{pSIC} = \left(1-P_{D_1}^{pSIC}\right) R_1 + \left(1-P_{D_2}\right) R_2. \tag{20b}$$

5. NUMERICAL RESULTS

In this section, we numerically simulate some theoretical results from some figures to show the outage performance. In particular, main parameters can be seen in Table I. In addition, the Gauss-Chebyshev parameter is selected as $K = 150$ to yield a close approximation.

Figure 2 demonstrates the OP versus transmit SNR of the proposed model in presence of ideal and imperfections at SIC. As we can clearly observe that as the imperfections reduce, the performance of the of the user increasing comparatively. The far user has the better performance compared to near user in both the cases, because the power allocation to the far user is highest. Also the simulations indicate that analytical and

Table 1. System parameters used in the performance evaluation.

System Parameters	Values
Monte Carlo simulations repeated	10^7 iterations
The power allocation coefficients	$\{\nu_1, \nu_2\} = \{0.2, 0.8\}$
The target rate at D_1	$R_1 = 1$ bps/Hz
The target rate at D_2	$R_2 = 0.5$ bps/Hz
The interference signal channel power gains	$\lambda_I = 0.01$
The channel estimation error	$\Omega_e = 0.01$
The mean value of $10\log\left(\lvert h_i\rvert^2\right)$	$\mu_{g_1} = \mu_{g_2} = 4$ dB
The standard deviation of $10\log\left(\lvert \sigma_{g_i}\rvert^2\right)$	$\sigma_{g_1} = \sigma_{g_2} = 5$ dB

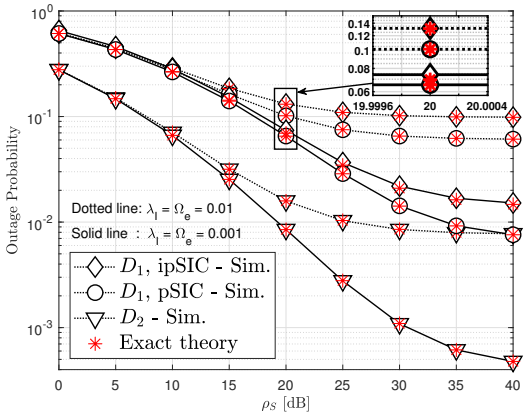

Figure 2. Outage Probability versus transmit SNR in presence of imperfections

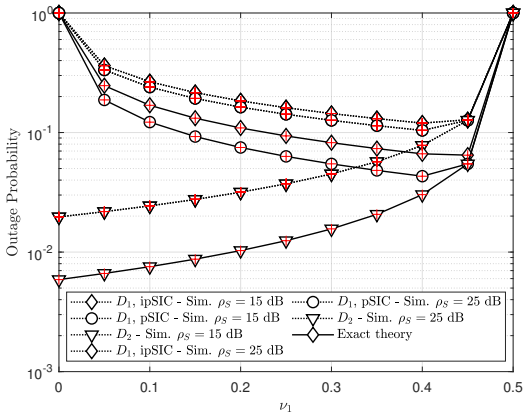

Figure 3. Outage Probability versus v_1, with $\lambda_I = \Omega_e = 0.01$

exact simulations are tightly packed with each other which verifies the correctness of the obtained expressions in section 3.

Figure 3 shows the simulation between OP versus power allocation at D_1 for fixed level of imperfections in the system, which can be considered negligible. As we can observe, as the power level increases for D_1, the performance of the user increases and the performance of D_2 reduces simultaneously. This is because the power allocation in NOMA follows the condition $v_1 + v_2 = 1$. As the power allocation becomes equal for both users at $v_1 = v_2 = 0.5$, the performance of both users becomes equal and the curves converges at the particular point. Another important point to be noticed is the effect of transmit SNR. As we can observe a huge gap between the curves, this is because of the change in transmit SNR. As the transmit SNR increases, the quality of signal transmission increases, leading to better outage probability for the user.

In similar to figure 3, figure 4 demonstrates the simulation between OP and different levels of target rates assigned to the users in the network. The analysis was performed for two different transmit SNR values. We can observe that D_2 has shown better performance for overall simulation because of the highest power allocation to it. Whereas at D_1, the perfect and imperfect SIC levels are considered with minute difference and the change in the performance can be observed clearly. The maximum target rate of the system is 2 and the performance of the users increases comparatively as we reduce the target rates. As the transmit SNR increases, the performance of the users in all scenarios increases as it shows the quality of signal transmitting.

Finally, figure 5 demonstrates the throughput performance of the system for various levels of imperfections, keeping the target rate at maximum for both the users. As we can observe from the system, with the level of imperfections increasing, the throughput performance of the system is decreasing rapidly. The observation shows that though the increased imperfections are noticeable, the change of the performance is stable which indicates that ability of fading distribution to compensate the effects. Also the transmit SNR play vital role, as the transmit SNR increases, the performance changes for the scenarios.

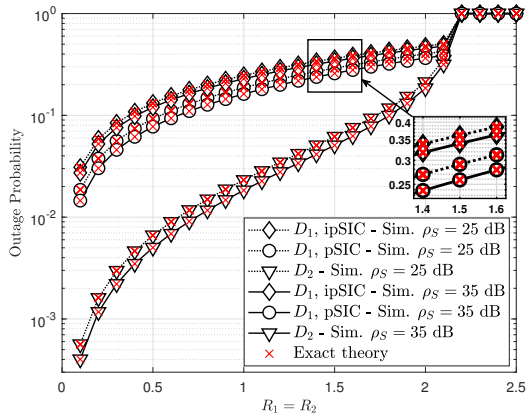

Figure 4. Outage Probability versus R_1=R_2, with $\lambda_I = \Omega_e = 0.01$, $\nu_1 = 0.05$ and $\nu_2 = 0.95$

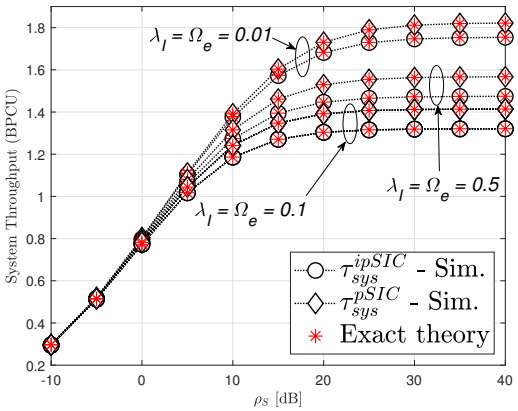

Figure 5. ..., with $\nu_1 = 0.05$, $\nu_2 = 0.95$ and $R_1 = R_2 = 2$

6. CONCLUSION

In this paper, we have considered a NOMA network with two users D_1 and D_2 over log-normal fading distribution. The considered model is expected to be facing imperfections in CSI and SIC. The performance was analysed in terms of outage probability and throughput of the system. The obtained expressions are simulated in aid with Monte-Carlo method, to verify the correctness of computations, and the simulations shows that the analytical and simulation are tightly packed with each other. From the simulation analysis, it can be clearly understood that the transmit SNR and power allocation to the user play a pivotal role in enhancing the performance of users. The role of imperfections are also shown in the simulations where, for minute change in the level of imperfection, the change in performance is also considerably observable. Finally, the proposed model has shown significant performance compared to other system models in various researches over different fading distributions and with the presence of imperfections.

REFERENCES

[1] Y. Saito, Y. Kishiyama, A. Benjebbour, T. Nakamura, A. Li and K. Higuchi, "Non-Orthogonal Multiple Access (NOMA) for Cellular Future Radio Access," in *IEEE 77th Vehicular Technology Conference (VTC Spring)*, 2013, pp. 1-5, doi: 10.1109/VTCSpring.2013.6692652.

[2] D. Wan, M. Wen, F. Ji, Y. Liu and Y. Huang, "Cooperative NOMA Systems With Partial Channel State Information Over Nakagami-m Fading Channels," in *IEEE Transactions on Communications*, vol. 66, no. 3, pp. 947-958, March 2018, doi: 10.1109/TCOMM.2017.2772273.

[3] R. Jiao, L. Dai, J. Zhang, R. MacKenzie and M. Hao, "On the Performance of NOMA-Based Cooperative Relaying Systems Over Rician Fading Channels," in *IEEE Transactions on Vehicular Technology*, vol. 66, no. 12, pp. 11409-11413, Dec. 2017, doi: 10.1109/TVT.2017.2728608.

[4] F. Kara and H. Kaya, "BER performances of downlink and uplink NOMA in the presence of SIC errors over fading channels", *IET Communications*, vol. 12, no. 15, 1834-1844, 2018.

[5] Y. Yin, Y. Peng, M. Liu, J. Yang and G. Gui, "Dynamic User Grouping-Based NOMA Over Rayleigh Fading Channels," in *IEEE Access*, vol. 7, pp. 110964-110971, 2019, doi: 10.1109/ACCESS.2019.2934111.

[6] P. Sharma, A. Kumar and M. Bansal, "Performance analysis of downlink NOMA over $\eta - \mu$ and $\kappa - \mu$ fading channels". *IET Commun.*, vol. 14, no. 3, 522-531, 2020.

[7] R. R. Kurup, S. Mahin, M. Sandhyana, R. Dev M., V. Priyanka and A. V. Babu, "Outage Performance of Cooperative NOMA System in Log-Normal Fading Channels," in *IEEE International Conference on Electronics, Computing and Communication Technologies (CONECCT)*, 2020, pp. 1-6, doi: 10.1109/CONECCT50063.2020.9198393.

[8] R. K. Ahiadormey, P. Anokye, H. -S. Jo, C. Song and K. -J. Lee, "Secrecy Outage Analysis in NOMA Power Line Communications," in *IEEE Communications Letters*, vol. 25, no. 5, pp. 1448-1452, May 2021, doi: 10.1109/LCOMM.2021.3057080.

[9] M. Elhattab, M. A. Arfaoui, C. Assi and A. Ghrayeb, "Reconfigurable Intelligent Surface Enabled Full-

Duplex/Half-Duplex Cooperative Non-Orthogonal Multiple Access," in *IEEE Transactions on Wireless Communications*, 2021, doi: 10.1109/TWC.2021.3120989.

[10] M. Elamassie, L. Bariah, M. Uysal, S. Muhaidat and P. C. Sofotasios, "Capacity Analysis of NOMA-Enabled Underwater VLC Networks," in *IEEE Access*, 2021, doi: 10.1109/ACCESS.2021.3122399.

[11] Y. Cao et al., "Joint User Grouping and Power Optimization for Secure mmWave-NOMA System," in *IEEE Transactions on Wireless Communications*, 2021, doi: 10.1109/TWC.2021.3120268.

[12] H. Lei, C. Zhu, K. -H. Park, W. Lei and I. S. Ansari, "On Secure Downlink NOMA Systems with Aerial Eavesdroppers," in *IEEE 32nd Annual International Symposium on Personal, Indoor and Mobile Radio Communications (PIMRC)*, 2021, pp. 733-738, doi: 10.1109/PIMRC50174.2021.9569589.

[13] M. Fu, Y. Zhou, Y. Shi and K. B. Letaief, "Reconfigurable Intelligent Surface Empowered Downlink Non-Orthogonal Multiple Access," in *IEEE Transactions on Communications*, vol. 69, no. 6, pp. 3802-3817, June 2021, doi: 10.1109/TCOMM.2021.3066587.

[14] G. Yang, X. Xu, Y. -C. Liang and M. D. Renzo, "Reconfigurable Intelligent Surface-Assisted Non-Orthogonal Multiple Access," in *IEEE Transactions on Wireless Communications*, vol. 20, no. 5, pp. 3137-3151, May 2021, doi: 10.1109/TWC.2020.3047632.

[15] Y. Cheng, K. H. Li, Y. Liu, K. C. Teh and G. K. Karagiannidis, "Non-Orthogonal Multiple Access (NOMA) with Multiple Intelligent Reflecting Surfaces," in *IEEE Transactions on Wireless Communications*, 2021, doi: 10.1109/TWC.2021.3081423.

[16] W. U. Khan, F. Jameel, N. Kumar, R. Jäntti and M. Guizani, "Backscatter-Enabled Efficient V2X Communication With Non-Orthogonal Multiple Access," in *IEEE Transactions on Vehicular Technology*, vol. 70, no. 2, pp. 1724-1735, Feb. 2021, doi: 10.1109/TVT.2021.3056220.

[17] E. N. Tominaga, H. Alves, R. D. Souza, J. Luiz Rebelatto and M. Latva-aho, "Non-Orthogonal Multiple Access and Network Slicing: Scalable Coexistence of eMBB and URLLC," in *IEEE 93rd Vehicular Technology Conference (VTC2021-Spring)*, 2021, pp. 1-6, doi: 10.1109/VTC2021-Spring51267.2021.9448942.

[18] D.-T. Do, M. Vaezi, and T.-L. Nguyen, "Wireless powered cooperative relaying using NOMA with imperfect CSI," in *Proc. IEEE Globecom Workshops*, Abu Dhabi, United Arab Emirates, pp. 1-6, Dec. 2018.

[19] V. N. Vo, C. So-In, H. Tran, D.-D. Tran, S. Heng, P. Aimtongkham, and A.-N. Nguyen, "On security and throughput for energy harvesting untrusted relays in IoT systems using NOMA," *IEEE Access*, vol. 7, pp. 149341-149354, 2019.

[20] D.-T. Do, T.-L. Nguyen, K. M. Rabie, X. Li, and B. M. Lee, "Throughput analysis of multipair two-way replaying networks with NOMA and imperfect CSI," *IEEE Access*, vol. 8, pp. 128942–128953, 2020.

[21] D.-T. Do, T. Anh Le, T. N. Nguyen, X. Li, and K. M. Rabie, "Joint impacts of imperfect CSI and imperfect SIC in cognitive radio-assisted NOMA-V2X communications," *IEEE Access*, vol. 8, pp. 128629-128645, 2020.

[22] D. T. Do, T. T. T. Nguyen, C. B. Le, and J. W. Lee, "Two-way transmission for low-latency and high-reliability 5G cellular V2X communications," *Sensors*, vol. 20, no. 2, p. 386, 2020.

[23] Kurup, Radhika R., et al. "Outage Performance of Cooperative NOMA System in Log-Normal Fading Channels," In *IEEE International Conference on Electronics, Computing and Communication Technologies (CONECCT)*, pp. 1-6, 2020.

[24] I. S. Gradshteyn and I. M. Ryzhik, *Table of Integrals, Series and Products*, 6th ed. New York, NY, USA: Academic Press, 2000.

[25] X. Yue, Y. Liu, S. Kang, A. Nallanathan, and Y. Chen, "Modeling and analysis of two-way relay non-orthogonal multiple access systems," *IEEE Trans. Commun.*, vol. 66, no. 9, pp. 3784-3796, Sep. 2018.

[26] M. Abramowitz and I. Stegun, *Handbook of Mathematical Functions with Formulas, Graphs, and Mathematical Tables*, New York, NY, USA: Dover, 1972.